Iranian Journal of Numerical Analysis and Optimization
Vol. 16, No. 4, 2026, pp 1189–1220
https://doi.org/10.22067/ijnao.2026.97008.1804
https://ijnao.um.ac.ir/

Research Article

A semi-analytical study on Hepatitis A virus transmission in Indonesia

A. Maheswari, V. Ananthaswamy*, and J. Anantha Jothi

Abstract

A mathematical layout that depicts the epidemiology of Hepatitis A in Indonesia is analyzed in the present research. The framework's specific four compartments —Susceptible, individuals, treatment, and recovered are resolved approximate analytically through the Laplace Adomian decomposition technique and Taylors series method. For each of the four compartments, the approximate analytical answers are stated. The outcomes of multiple kinds of model parameters are demonstrated graphically. The numerical simulation (MATLAB) and our approximate analytical outcomes are contrasted and provided in the table. The approximate analytical outcomes and the numerical simulation fit each other precisely.

AMS subject classifications (2020): 34A05, 34A12, 34E05, 34E10.

*Corresponding author

Received 15 December 2025; revised 4 February 2026; accepted 7 April 2026

Alagarsamy Maheswari
Department of Mathematics, Velammal College of Engineering and Technology, Madurai, Tamil Nadu, India. e-mail: ama@vcet.ac.in

Vembu Ananthaswamy
Research Centre and PG Department of Mathematics, The Madura College (Affiliated to Madurai Kamaraj University), Madurai, Tamil Nadu, India. e-mail: ananthu9777@gmail.com

Jeya Kumar Anantha Jothi
Research Scholar, Research Centre and PG Department of Mathematics, The Madura College (Affiliated to Madurai Kamaraj University), Madurai, Tamil Nadu, India. e-mail:ananthajothij98@gmail.com

How to cite this article
Maheswari, A., Ananthaswamy, V. and Anantha Jothi, J., A semi-analytical study on Hepatitis A virus transmission in Indonesia. *Iran. J. Numer. Anal. Optim.*, 2026; 16(4): 1189-1220. https://doi.org/10.22067/ijnao.2026.97008.1804

Keywords: Hepatitis A virus (HAV), $SITR$ model, Nonlinear initial value problem, Laplace Adomian decomposition method (LADM), Taylors series method (TSM), Numerical simulation.

1 Introduction

Acute, transient liver infections are caused by the Hepatitis A virus (HAV) and are typically contracted by the fecal-oral route from tainted beverages or food. The signs and symptoms can include fatigue, nausea, and jaundice, but many people do not experience any of them. Once antibodies are formed, the body's defense system offers lifetime protection, and the infection is typically not persistent. When any individual consumes food or water tainted by an infected person's excrement, it might spread. Hygiene and sanitation deficiencies (e.g., filthy and unwashed hands) and an inadequate supply of potable water are linked to the risk of contracting HAV. For the avoidance of HAV, a vaccine has been developed that is effective as well as secure. Vaccination and proper hygienic are part of safeguarding.

For the sake of the computational estimation of nonlinear and linear stochastic and predictable epidemics incorporating treatment cure and partial immunity, Arif, Abodayeh, and Nawaz [4] introduced and examined a novel finite difference technique. The purpose of the Bae et al. [6] inquiry was to examine HAV persistence on six distinct food-contact surfaces: wood, glass, stainless steel, ceramic, rubber, and plastic. Additionally, it offers helpful information for preventing food-borne illness and controlling HAV on various surfaces that handle food. According to Fiore's research [12], epidemics of Hepatitis A (HA) that are transmitted by food or water are not common in the United States. Nevertheless, people who handle food with HA are often recognized, and assessing their immunoprophylactic needs and putting control measures in place as a significant strain on public health services. In order to determine the epidemiological features of HA cases that take place at High School X as well as the risk variables, Harisma et al. [17] conducted an observational study using a cross-sectional methodology. Ilahi and Fadilaturrohmah [20] presented a mathematical framework that provided a different perspective on how the Hepatitis C virus (HCV) spreads while in medical care in a population with a chronic infection. Sensitivity analysis was required to establish parameters for treating HCV and illness prevention. The risk factors for developing fulminant hepatitis and fatality in Mexico were examined by MacKinney-Novelo et al. [24]. The susceptible-infected-treatment-recovered (SITR) scheme for the dissemination of HA by vaccination was covered in the Sidik, Sari, and Ismail's study [32]. Additionally, the stability with respect to the model for the transmission of HA disease around the sites was examined, along with the interpretation of the model created

through numerical simulations and the analysis of the impact of treatment and vaccination on the human population sick with HA.

People with untreated chronic liver disease have a higher chance of dying. The virus can be transmitted from person to person by the oral route of faeces, by medication delivery in the vein [23, 34, 35], or by consuming tainted food or beverages. Transmission can also occur through routine contact with blood or its components that contain HAV, but not with urine or saliva. According to Staes et al. [33], babies and asymptomatic, nonjaundiced HAV-infected persons are the main sources of HAV dissemination. According to research by Bianco et al. [8], travel is a second common cause of infection in areas with high infection rates, where dissemination can occur both directly and indirectly. According to Koff [22], jaundice, light-colored faces, or dark-colored urine may be signs of HAV at the onset of clinical symptoms or within a day or two of them.

Many mathematical models that describe the processes of HAV dispersion have been established, produced, and analyzed in an attempt to avoid the disease. Guimaraens and Codec [15] created a susceptible-infectious-recovery (SIR) mathematical structure to examine how the epidemiologic dynamics of HA are affected by different infection treatments. Van Effelterre, Marano, and Jacobsen [36] created a mathematical structure called susceptible, latent, infectious, and recovered immune (S-L-I-R) to highlight the importance of considering herd protection caused by early childhood HA immunization. The Fiore, Wasley, and Bell [13] model supported the Immunization Practices Advisory Committee's recommendations for the universal HA vaccination of one-year-olds. Ajelli et al. [1] developed the basic mathematical foundation for the seasonal variations of HAV in regions of Italy with respect to a moderate epidemic status in another study. Similarly, Ajelli et al. [2] developed an individual-based model that was parameterized employing the sociodemographic data and epidemiological and featured an active network of links that comprised millions of humans. The findings from the study indicate that the inadequate vaccination proportion in Italy is adequate to prevent the spread of HA. The Van Effelterre et al. [37] investigation proposed a method that provides insight into the new HAV epidemiology and may be implemented to evaluate the impact of vaccination and other public health initiatives in various settings.

Researchers were also recently investigated the dynamics and outcomes related to a vaccination option that contains HA contamination [5, 9]. For instance, the findings of Brouwer et al. [9] developed a mathematical representation of HAV transmission to assess local spread trends and the effect of vaccination upon the severity and durability of the HAV dissemination in Michigan. They also calculated the proportion of instances that the immunization program prevented in Southeast Michigan and the remaining areas of the state. For the HAV pandemic, Van

Effelterre et al. [37] created and addressed a linear age-organized SEIAR (susceptible-exposed-symptomatic-asymptomatic-recovered) subdivision model.

The research of Febriyanto and Dewi [11] served as the motivation for this work. However, their research, which incorporated the 14th order Runge-Kutta (R-K 14th) approach in MATLAB which lacks the approximate solutions in explicit and did not account for the effect of different model parameter values on HAV control. In order to fill the gap, we used an approximate analytical method and provided the solutions in explicit form. Also, we compared our approximate analytical solutions with the numerical simulation. Therefore, the primary objective of this work was to find the approximate analytical outcomes of the dynamic deterministic epidemiological framework that considers and graphically depicts the influence of several parameters. While other academics now handle these kinds of issues with implicit answers, our semi-analytical results offer explicit expressions. The semi-analytical findings and numerical simulation are subsequently contrasted and graphically shown. We employ numerical simulation, which shows a very good fit to the precision of our method.

The selection of the Laplace Adomian decomposition method (LADM) and Taylors series method (TSM) in this study is based on the need for accuracy of the results with the simulation of the SITR model, which is nonlinear. This method can solve a set of differential equations (DEs) with high precision, especially for short spans of time intervals, making it suitable for predicting the dynamics of infectious diseases over a certain period. Also, these methods provide a much smaller truncation error with the numerical simulation results.

2 Mathematical overview of the problem

The $SITR$ model, which was created by splitting the human population into four categories based on reference sources about mathematical modeling of infectious illnesses is used to explain how vaccination spreads HA disease. The population contains Susceptible (S), a population of healthy people who are at risk for experiencing HA; Infected (I), a group of people who have HA at the moment; Treatment (T), a community of people receiving medical care; and Recovery (R), a group of people that are immune to HA who have recovered. The following presumptions guided the development of the $SITR$ framework to simulate the transmission of HA illness. Populations never change.

a) Because the persons born belong to susceptible groups and each person who passes away has a proportionate rate with other groups, both the birth and death rates are equal. People with an infection or HA will go through the treatment procedures.

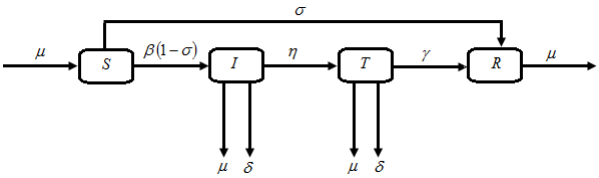

Figure 1: Schematic of the Hepatitis model ($SITR$) a vaccination-related spread

b) The infected and treatment class experienced a death yesterday due to HA infection, but the Susceptible and Recovery squad experienced a natural death.

c) Immunization of infants or kids.

d) HA infection is a possibility for the susceptible individual group.

e) When vulnerable people come into contact with infected people or the virus comes into contact with susceptible people, HA can spread.

f) After getting treatment, people will recover from HA.

g) Only one illness, HA spreads in this situation.

h) Those who recover may be able to spread the infection again.

The mathematical framework for the propagation of HA illness is derived from these hypotheses and is displayed in Figure 1.

Figure 1 provides the DE system for each compartment, which is as follows [11]:

$$\frac{dS}{d\tau} = \mu - (1-\alpha)(\beta)S\frac{1}{N} - \alpha\, S - \mu\, S, \tag{1}$$

$$\frac{dI}{d\tau} = (1-\alpha)(\beta)S\frac{1}{N} - \eta\, I - \delta\, I - \mu\, I, \tag{2}$$

$$\frac{dT}{d\tau} = \eta\, I - \gamma\, T - \delta\, T - \mu\, T, \tag{3}$$

$$\frac{dR}{d\tau} = \gamma\, T + \sigma\, S - \mu\, R. \tag{4}$$

To facilitate model analysis, the equation can be made simpler.

$$s = \frac{S}{N}, \quad i = \frac{I}{N}, \quad t = \frac{T}{N}, \quad r = \frac{R}{N}. \tag{5}$$

So that the governing equations may be found as follows:

$$\frac{ds}{d\tau} = \mu - (1-\sigma)(\beta)s\, i - \sigma\, s - \mu\, s, \tag{6}$$

$$\frac{di}{d\tau} = (1-\alpha)(\beta)s\, i - \eta\, i - \delta\, i - \mu\, i, \tag{7}$$

$$\frac{dt}{d\tau} = \eta\, i - \gamma\, t - \delta\, t - \mu\, t, \tag{8}$$

$$\frac{dr}{d\tau} = \gamma\, t + \sigma\, s - \mu\, r. \tag{9}$$

The corresponding initial circumstances are

$$\left.\begin{aligned} &At \qquad \tau = 0, \quad s(0) = A = 0.8, \quad i(0) = B = 0.2, \\ &t(0) = D = 0.0, \quad r(0) = F = 0.0. \end{aligned}\right\} \tag{10}$$

We identified a subsequent set of values as the initial one for each compartment using the same data source that Febriyanto and Dewi [11] used: $s(0) = 0.8$, $i(0) = 0.2$, $t(0) = 0.0$, and $r(0) = 0.0$, additionally the following parameters were ascertained: $\mu = 0.02$, $\delta = 0.0025$, $\sigma = 0.008$, $\beta = 0.4286$ and $\eta = 0.3$.

3 Approximate analytical expression for the nonlinear initial value problems

DEs, both nonlinear and linear, have a significant influence on many scientific and technical fields and can be used to represent a wide range of behaviors. A number of first-order nonlinear ordinary differential equations (ODEs) lack adequate semi-analytical results. The variational iterative technique [28], Sumudu transform methodology [10], Sumudu Adomian decomposition approach [21], homotopy analysis technique [25, 26, 31], homotopy perturbation technique [3], new homotopy perturbation approach [29], differential transform methodology [16] and Laplace Adomian decomposition method [7, 25] are some of the semi-analytical techniques that can be used to precisely resolve first-order ODEs in nonlinear.

3.1 Approximate analytical expressions for (6) through (9) by employing Laplace Adomian decomposition technique

The LADM, which blends with the Laplace transform (LT) as well as the Adomian decomposition method (ADM), is a powerful mixed technique to deal with differential equations (DEs), especially ones with nonlinearity. Its use results in better precision and effectiveness as compared to traditional approaches. LADM provides several significant advantages by solving nonlinear

DEs without the need for linearization, discrimination, perturbation, or transformation. This attribute makes problem-solving easier and allows for more precise results. LADM delivers approximate analytical outcomes in the form of a fast convergent infinite power series with easily computed terms. Because of this feature, it can be used in a wide range of scientific and engineering disciplines [7, 25, 30]. Its efficacy is shown in several fields, such as fluid dynamics, heat transfer, population dynamics, and more, where LADM has lately been effectively applied to resolve difficult problems and yield useful data [30].

In this sub-section, we demonstrate the application of the LADM to nonlinear ordinary differential systems to attain the semi-analytical expressions. To initiate the process, we commence by applying the LT which is denoted by applying the Laplace transform L for both sides of (6)–(9), we attained

$$L(s) = s(0) + L(\mu) - (1-\sigma)\beta\, L(s\, i) - (\sigma+\mu)L(s), \tag{11}$$

$$L(i) = i(0) + (1-\sigma)\beta\, L(s\, i) - (\eta+\delta+\mu)L(i), \tag{12}$$

$$L(t) = t(0) + \eta\, L(i) - (\gamma+\delta+\mu)L(t), \tag{13}$$

$$L(r) = r(0) + \gamma\, L(t) + \sigma\, L(s) - \mu\, L(r). \tag{14}$$

Assuming that the answers to s, i, t, and r may be represented as infinite series, we proceed.

Additionally, we use Adomian polynomials, whose properties are stated as follows, to split up the nonlinear terms included $s\, i = V$ in the model:

$$s = \sum_{n=0}^{\infty} s_n,\ \ i = \sum_{n=0}^{\infty} i_n,\ \ t = \sum_{n=0}^{\infty} t_n,\ \ r = \sum_{n=0}^{\infty} r_n,\ \ V = \sum_{n=0}^{\infty} V_n(s,\, i). \tag{15}$$

The Adomian polynomials represented by V_n, are described as follows:

$$V_n = \frac{1}{n!}\frac{d^n}{d\lambda^n}\left[\sum_{i=0}^{\infty}\lambda^i s_i \sum_{i=0}^{\infty}\lambda^i i_i\right], \tag{16}$$

$$V_0 = s_0 i_0, \tag{17}$$

$$V_1 = s_1 i_0 + s_0 i_1. \tag{18}$$

Equations (15) through (18) can be substituted into (11) through (14), yielding

$$L\left(\sum_{n=0}^{\infty} s_n\right) = s(0) + L(\mu) - (1-\sigma)\beta\, L\left(\sum_{n=0}^{\infty} V_n(s,\, i)\right) - (\sigma+\mu)L\left(\sum_{n=0}^{\infty} s_n\right), \tag{19}$$

$$L\left(\sum_{n=0}^{\infty} i_n\right) = i(0) + (1-\sigma)\beta\, L\left(\sum_{n=0}^{\infty} V_n(s,i)\right) - (\eta+\delta+\mu)L\left(\sum_{n=0}^{\infty}\right), \tag{20}$$

$$L\left(\sum_{n=0}^{\infty} t_n\right) = t(0) + \eta L\left(\sum_{n=0}^{\infty} i_n\right) - (\gamma+\delta+\mu)\, L\left(\sum_{n=0}^{\infty} t_n\right), \tag{21}$$

$$L\left(\sum_{n=0}^{\infty} r_n\right) = r(0) + \gamma\left(\sum_{n=0}^{\infty} t_n\right) + \sigma L\left(\sum_{n=0}^{\infty} s_n\right) - \mu L\left(\sum_{n=0}^{\infty} r_n\right). \tag{22}$$

The specific properties of the LT derivative are offered by

$$wL(\overline{U}) - \overline{U}(0) = L(\overline{G}(\overline{U})), \tag{23}$$

$$L(\overline{U}) = \frac{1}{w}\overline{U}(0) + \frac{1}{w}L(\overline{G}(\overline{U})). \tag{24}$$

Utilizing the characteristics provided in (24) in (19) through (22), we attain

$$L\left(\sum_{n=0}^{\infty} s_n\right) = \frac{1}{w}s(0) + \frac{1}{w}L(\mu) - \frac{1}{w}(1-\sigma)\beta L\left(\sum_{n=0}^{\infty} V_n(s,i)\right) - \frac{1}{w}(\sigma+\mu)L\left(\sum_{n=0}^{\infty} s_n\right), \tag{25}$$

$$L\left(\sum_{n=0}^{\infty} i_n\right) = \frac{1}{w}i(0) + \frac{1}{w}(1-\sigma)\beta L\left(\sum_{n=0}^{\infty} V_n(s,i)\right) - \frac{1}{w}(\eta+\delta+\mu)L\left(\sum_{n=0}^{\infty} i_n\right), \tag{26}$$

$$L\left(\sum_{n=0}^{\infty} t_n\right) = \frac{1}{w}t(0) + \frac{1}{w}\eta L\left(\sum_{n=0}^{\infty} i_n\right) - \frac{1}{w}(\gamma+\delta+\mu)L\left(\sum_{n=0}^{\infty} t_n\right), \tag{27}$$

$$L\left(\sum_{n=0}^{\infty} r_n\right) = \frac{1}{w}r(0) + \frac{1}{w}\gamma L\left(\sum_{n=0}^{\infty} t_n\right) + \frac{1}{w}\sigma L\left(\sum_{n=0}^{\infty} s_n\right) - \frac{1}{w}\mu L\left(\sum_{n=0}^{\infty} r_n\right). \tag{28}$$

The LADM's zeroth iteration for (25) through (28) is outlined below:

$$L(s_0) = \frac{1}{w}s(0), \tag{29}$$

$$L(i_0) = \frac{1}{w}i(0), \tag{30}$$

$$L(t_0) = \frac{1}{w}t(0), \tag{31}$$

$$L(r_0) = \frac{1}{w} r(0). \tag{32}$$

Now that we have applied the inverse LT to (29) through (32) and replaced (10), we acquire

$$s_0 = A, \tag{33}$$
$$i_0 = B, \tag{34}$$
$$t_0 = D, \tag{35}$$
$$r_0 = F. \tag{36}$$

The LADM's first iteration for (25) through (28) is obtained through contrasting the equation's two sides:

$$L(s_1) = \frac{1}{w} L(\mu) - \frac{1}{w}(1-\sigma)\beta L(V_0(s,i)) - \frac{1}{w}(\sigma+\mu)L(s_0), \tag{37}$$
$$L(i_1) = \frac{1}{w}(1-\sigma)\beta L(V_0(s,i)) - \frac{1}{w}(\eta+\delta+\mu)L(i_0), \tag{38}$$
$$L(t_1) = \frac{1}{w}\eta L(i_0) - \frac{1}{w}(\gamma+\delta+\mu)L(t_0), \tag{39}$$
$$L(r_1) = \frac{1}{w}\gamma L(t_0) + \frac{1}{w}\sigma L(s_0) - \frac{1}{w}\mu L(r_0). \tag{40}$$

The inverse LT are now being applied for (37)–(40) and putting (33)–(36), we get

$$s_1 = [\mu - (1-\sigma)\beta AB - (\sigma+\mu)A]\,\tau, \tag{41}$$
$$i_1 = [(1+\sigma)\beta AB - (\eta+\delta+\mu)B]\,\tau, \tag{42}$$
$$t_1 = [\eta B - (\gamma+\delta+\mu)D]\,\tau, \tag{43}$$
$$r_1 = [\gamma D + \sigma A - \mu F]\,\tau. \tag{44}$$

The second iteration for (25)–(28) of the LADM is attained by compare both sides of the equation, we get

$$L(s_2) = -\frac{1}{w}(1-\sigma)\beta L(V_1(s,i)) - \frac{1}{w}(\sigma+\mu)L(s_1), \tag{45}$$
$$L(i_2) = \frac{1}{w}(1-\sigma)\beta L(V_1(s,i)) - \frac{1}{w}(\eta+\delta+\mu)L(i_1), \tag{46}$$
$$L(t_2) = \frac{1}{w}\eta L(i_1) - \frac{1}{w}(\gamma+\delta+\mu)L(t_1), \tag{47}$$
$$L(r_2) = \frac{1}{w}\gamma L(t_1) + \frac{1}{w}\sigma L(s_1) - \frac{1}{w}\mu L(r_1). \tag{48}$$

Now, taking inverse LT for (45)–(48) and replaced (41)–(44), we get

$$
\begin{aligned}
s_2 =& \left[-(1-\sigma)\beta\left(A((1+\sigma)\beta AB-(\eta+\delta+\mu)B)\right)\right]\frac{\tau^2}{2!}\\
&-(1-\sigma)\beta(B(\mu-(1-\sigma)\beta AB-(\sigma+\mu)A))\frac{\tau^2}{2!}\\
&-(\sigma+\mu)(\mu-(1-\sigma)\beta AB-(\sigma+\mu)A)\frac{\tau^2}{2}, \qquad (49)\\
i_2 =& \left[(1-\sigma)\beta\left(A((1+\sigma)\beta AB-(\eta+\delta+\mu)B)\right)\right]\\
&+(1-\sigma)\beta(B(\mu-(1-\sigma)\beta AB-(\sigma+\mu)A))\frac{\tau^2}{2!}\\
&+(-(\eta+\delta+\mu)(1+\sigma)\beta AB-(\eta+\delta+\mu)B)\frac{\tau^2}{2!}, \qquad (50)\\
t_2 =& \left[\eta((1+\sigma)\beta AB-(\eta+\delta+\mu)B)\right]\frac{\tau^2}{2!}\\
&-\left[(\gamma+\delta+\mu)(\eta B-(\gamma+\delta+\mu)D)\right]\frac{\tau^2}{2!}, \qquad (51)\\
r_2 =& \left[\gamma(\eta B-(\gamma+\delta+\mu)D)-\sigma(\mu-(1-\sigma)\beta AB-(\sigma+\mu)A)\right]\frac{\tau^2}{2!}\\
&-\left[\mu(\gamma D+\sigma A-\mu F)\right]\frac{\tau^2}{2!}. \qquad (52)
\end{aligned}
$$

A similar methodology can then be used to calculate the remaining terms. The responses to the aforementioned systems can be roughly represented as an infinite series using these computed values in the manner described below:

$$s = s_0 + s_1 + s_2 + \cdots, \qquad (53)$$

$$i = i_0 + i_1 + i_2 + \cdots, \qquad (54)$$

$$t = t_0 + t_1 + t_2 + \cdots, \qquad (55)$$

$$r = r_0 + r_1 + r_2 + \cdots. \qquad (56)$$

Thus, by replacing (33)–(36), (41)–(44), and (49)–(52) into (53)–(56), we obtain the approximate analytical expressions of (6)–(9). The findings are as follows:

$$
\begin{aligned}
s =& A+\left[\mu-(1-\sigma)\beta AB-(\sigma+\mu)A\right]\tau\\
&+\left[-(1-\sigma)\beta\left(A((1+\sigma)\beta AB-(\eta+\delta+\mu)B)\right)\right]\frac{\tau^2}{2!}\\
&+\left[-(1-\beta)(B(\mu-(1-\sigma)\beta AB-(\sigma+\mu)A))\right]\frac{\tau^2}{2!}\\
&+\left[-(\sigma+\mu)(\mu-(1-\sigma)\beta AB-(\sigma+\mu)A)\right]\frac{\tau^2}{2!}, \qquad (57)\\
i =& B+\left[(1+\sigma)\beta AB-(\eta+\delta+\mu)B\right]\tau
\end{aligned}
$$

$$+\left[(1-\sigma)\beta\left(A((1+\sigma)\beta AB-(\eta+\delta+\mu)B)\right)\right]\frac{\tau^2}{2!}$$
$$+\left[(1-\sigma)\beta\left(B(\mu-(1-\sigma)\beta AB-(\sigma+\mu)A)\right)\right]\frac{\tau^2}{2!}$$
$$+\left[-(\eta+\delta+\mu)(1+\sigma)\beta AB-(\eta+\delta+\mu)B\right]\frac{\tau^2}{2!}, \tag{58}$$

$$t = D+\left[\eta B-(\gamma+\delta+\mu)D\right]\tau$$
$$+\left[\eta((1+\sigma)\beta AB-(\eta+\delta+\mu)B)\right]\frac{\tau^2}{2!}$$
$$+\left[-(\gamma+\delta+\mu)(\eta B-(\gamma+\delta+\mu)D)\right]\frac{\tau^2}{2!}, \tag{59}$$

$$r = F+\left[\gamma D+\sigma A-\mu F\right]\tau$$
$$+\left[\gamma(\eta B-(\gamma+\delta+\mu)D)-\sigma(\mu-(1-\sigma)\beta AB-(\sigma+\mu)A)\right]\frac{\tau^2}{2!}$$
$$-\left[\mu(\gamma D+\sigma A-\mu F)\right]\frac{\tau^2}{2!}. \tag{60}$$

3.2 Approximate analytical expressions for (6) through (9) by employing Taylor's series approach

One of the easiest and most efficient ways to handle nonlinear equations is the TSM [14, 18, 19, 27]. Furthermore, because it doesn't require an extensive knowledge in mathematical analyzing, TSM is available to a wider range of researchers. Even though there may be certain challenges when applying TSM, such as when dealing with strong nonlinear DEs, these challenges can typically be overcome by employing additional derivatives, obtaining polynomials with higher degree, or adopting the Padé approximant. TSM was employed to provide a structured and quantitative framework for evaluating the study parameters. Its selection is justified by its ability to multiple criteria into a coherent analytical process, ensuring consistency, objectivity, and reproducibility of the results. TSM has been selected deliberately to address the need for a systematic and objective evaluation framework. Compared to alternative approaches, TSM offers improved consistency in multi-criteria assessment and minimizes subjective bias, thereby strengthening the methodological rigor of the study. Its application ensures reliable evaluation and strengthens the robustness of the methodological approach. In this work, there is a complication occurred in solving the nonlinear term. To overcome this situation TSM has been used. In TSM we substitute the initial conditions in the nonlinear term to reduce the complications within three iterations the solution are converges faster. Nonlinear ordinary and fractional DEs, including

Lane-Emden [18], third-order boundary value issues, fractional Bratu-type equations [19], and nonlinear oscillator issues [27], have been extensively solved with TSM in the past few decades.

In this sub-section, we demonstrate the application of the TSM to nonlinear ordinary differential systems to attain the semi-analytical expressions. To initiate the process, for (6) through (9), the extension of the Taylor series is expressed as follows:

$$s(\tau) = \left[\sum_{a=0}^{2} \frac{d^a s}{d\tau^a}\right]_{\tau=0} \frac{\tau^a}{a!} = s(0) + \frac{s'(0)}{1!}\tau + \frac{s''(0)}{2!}\tau^2, \tag{61}$$

$$i(\tau) = \left[\sum_{a=0}^{2} \frac{d^a i}{d\tau^a}\right]_{\tau=0} \frac{\tau^a}{a!} = i(0) + \frac{i'(0)}{1!}\tau + \frac{i''(0)}{2!}\tau^2, \tag{62}$$

$$t(\tau) = \left[\sum_{a=0}^{2} \frac{d^a t}{d\tau^a}\right]_{\tau=0} \frac{\tau^a}{a!} = t(0) + \frac{t'(0)}{1!}\tau + \frac{t''(0)}{2!}\tau^2, \tag{63}$$

$$r(\tau) = \left[\sum_{a=0}^{2} \frac{d^a r}{d\tau^a}\right]_{\tau=0} \frac{\tau^a}{a!} = r(0) + \frac{r'(0)}{1!}\tau + \frac{r''(0)}{2!}\tau^2. \tag{64}$$

By implementing the initial circumstance given in (10), the zeroth step for (61)–(64) for $a = 0$ is as follows:

$$s(0) = A, \tag{65}$$

$$i(0) = B, \tag{66}$$

$$t(0) = D, \tag{67}$$

$$r(0) = F. \tag{68}$$

The initial iteration of (61)–(64) for $a = 1$ through (65)–(68) is as follows:

$$s'(0) = \mu - (1-\sigma)\beta s(0)\, i(0) - (\sigma + \mu)s(0), \tag{69}$$

$$i'(0) = (1-\sigma)\beta\, s(0)\, i(0) - (\eta + \delta + \mu)i(0), \tag{70}$$

$$t'(0) = \eta\, i(0) - (\gamma + \delta + \mu)t(0), \tag{71}$$

$$r'(0) = \gamma\, t(0) + \sigma\, s(0) - \mu\, r(0). \tag{72}$$

The second iterations of (61)–(64) for $a = 2$ applying (65)–(68) and (69)–(72) is as outlined below:

$$s''(0) = -(1-\sigma)\beta\,[s(0)i'(0) + s'(0)i(0)] - (\sigma + \mu)s'(0), \tag{73}$$

$$i''(0) = (1-\sigma)\beta\,[s(0)i'(0) + s'(0)i(0)] - (\eta + \delta + \mu)i'(0), \tag{74}$$

$$t''(0) = \eta i'(0) - (\gamma + \delta + \mu)t'(0), \tag{75}$$

$$r''(0) = \gamma t'(0) + \sigma\, s'(0) - \mu\, r'(0). \tag{76}$$

Adding (65)–(76), we attained the approximate analytical expressions for (6)–(9), which yields:

$$\begin{aligned} s(\tau) =& A + [\mu - (1-\sigma)\beta AB - (\sigma+\mu)A]\,\frac{\tau}{1!} \\ &+ [-(1-\sigma)\beta\,(A((1-\sigma)\beta AB - (\eta+\delta+\mu)B))]\,\frac{\tau^2}{2!} \\ &+ [-(1-\sigma)\beta\,(\mu - (1-\sigma)\beta AB - (\sigma+\mu)A)\,B]\,\frac{\tau^2}{2!} \\ &+ [-(\sigma+\mu)(\mu - (1-\sigma)\beta AB - (\sigma+\mu)A)]\,\frac{\tau^2}{2!}, \end{aligned} \tag{77}$$

$$\begin{aligned} i(\tau) =& B + [(1-\sigma)\beta AB - (\eta+\delta+\mu)B]\,\frac{\tau}{1!} \\ &+ [(1-\sigma)\beta\,(A((1-\sigma)\beta AB - (\eta+\delta+\mu)B))]\,\frac{\tau^2}{2!} \\ &+ [(1-\sigma)\beta\,((\mu - (1-\sigma)\beta AB - (\sigma+\mu)A))\,B]\,\frac{\tau^2}{2!} \\ &+ [-(\eta+\delta+\mu)((1-\sigma)\beta AB - (\eta+\delta+\mu)B)]\,\frac{\tau^2}{2!}, \end{aligned} \tag{78}$$

$$\begin{aligned} t(\tau) =& D + [\eta\beta - (\gamma+\delta+\mu)D]\,\frac{\tau}{1!} + [\eta((1-\sigma)\beta AB - (\eta+\delta+\mu)B)]\,\frac{\tau^2}{2!} \\ &+ [-(\gamma+\delta+\mu)(\eta B - (\gamma+\delta+\mu)D)]\,\frac{\tau^2}{2!}, \end{aligned} \tag{79}$$

$$\begin{aligned} r(\tau) =& F + [\gamma D + \sigma A - \mu F]\,\frac{\tau}{1!} + [\gamma(\eta B - (\gamma+\delta+\mu)B)]\,\frac{\tau^2}{2!} \\ &+ [\sigma(\mu - (1-\sigma)\beta AB - (\sigma+\mu)A) - \mu(\gamma D + \sigma A - \mu F)]\,\frac{\tau^2}{2!}. \end{aligned} \tag{80}$$

4 Numerical simulation

Additionally, the function maingraph in the program run in MATLAB has been employed to numerically resolve the above nonlinear DEs (6) to (9). The numerical simulation has been contrasted with the semi-analytical results. The MATLAB program listed in Appendix A. Figures 2–18 show the numerical simulation carried out using MATLAB, together with the approximate analytical expressions that were obtained by utilizing LADM and TSM. A fairly good consensus exists.

5 Results and discussions

By assigning each parameter to the appropriate value, Figure 2 illustrates the impact of general parameters, such as susceptible class, infected class, treatment, and recovered class. In this figures, we have compared our semi-analytical solutions LADM and TSM with the numerical solution (R-K 14^{th} approach) [11].

For susceptible class $s(\tau)$: Figures 3–4 and 11–12 displays the susceptible class $s(\tau)$ versus time τ by employing (57) and (77). Figures 3 and 11 interline that when the value of the vaccination effectiveness level σ, the transmission rate of an infected person to the suspect β raises, then the susceptible class get drops. From these we noted that the higher vaccine effectiveness σ increases immune protection and prevents individuals from remaining at risk, while a higher transmission rate β accelerates infection among nonimmune individuals together these mechanisms reduce the pool of susceptible individuals in the population. In figs. 4 and 12 interlines that the amount of the proportion of infected individuals who get medical care η raises so does the susceptible class. Therefore, an increase in the proportion of infected individuals receiving medical care η leads to earlier diagnosis, effective treatment, and isolation, which reduces disease transmission and allows fewer susceptible individuals to become infected therefore the susceptible class increases as more people remain uninfected.

For infected class $i(\tau)$: Figures 5–6 and 13–14 demonstrate the infected class $i(\tau)$ against time τ by utilizing (58) and (78). From these figs. 6 and 13, it depicts that the value for the both births or death rates that are not the outcomes of the HA sickness (naturally) μ, and the proportion of infected persons who got therapy η get raises then the infected class get falls. In general, an increase in the natural birth-death rate μ together with a higher proportion of infected individuals receiving therapy η reduces the number of infected individuals by removing infected persons through natural turnover and accelerating recovery through treatment, thereby causing the infected class to decline. Figures 5 and 14 show that as the amounts for the transmission rate of an infected individual to the vulnerable β increases, so does the infected class. Hence, when the transmission rate β increases, infected individuals spread the disease more efficiently, causing more people to become infected, so the infected class increases.

For treatment class $t(\tau)$: Figures 7–8 and 15–16 depict that the treatment class $t(\tau)$ with time τ via (59) and (79). Figures 8 and 16 reveal that the amount for the death rate due to HA infection δ, and the rate of recovery of a person after the medical care for HA infection γ get raised then the treatment class get drops. Form this we noted that the death rate from HA infection δ and the recovery rate after treatment γ increase, patients either die or recover faster, so fewer individuals remain in the treatment class, causing it to decrease. Figures 9–10 and 7 and 15, it exhibit that as the rate of transfer of an infected human to the vulnerable β and

proportion of infected individuals who got the medical care η increases so does the treatment class. Hence, when the infection spreads faster β and more infected individuals receive medical care η, more people enter treatment, so the treatment class increases.

For recovered class $r(\tau)$: Figures 9–10 and 17–18 highlight that the recovered class $r(\tau)$ versus time τ by using (60) and (80). Figures 9–10 and 17–18 it interline that the amount of vaccination effectiveness level σ, the proportion of infected individuals who receive treatment η, rate of recovery of an individual after undergoing treatment for HA infection γ raises then recovered class also get raises. From these we concluded that, when vaccine effectiveness σ improves, more infected individuals receive treatment η, and the recovery rate after treatment γ increases, more people gain immunity or recover from the infection, so the recovered class increases.

For Tables: The contrast for the numerical simulation between the LADM and TSM with the fixed quantities for the variables of vulnerable, diseased, medical care, and recovered is displayed in Tables 1 through 4. This table indicates that the average absolute error percentage was 0.1. The tables reveal that, on a comparatively small scale, our findings match well with the numerical simulation. Compared to our semi-analytical techniques, TSM was somewhat time-consuming, and evaluating values required more time than LADM. It is clear from analyzing the figures and tables that the LADM regularly offers a better approximation than the TSM with the simulations within the specified time interval. Nevertheless, even with a short time span, LADM successfully captures this behavior. This led us to conclude that the numerical simulation yields an approximation with greater precision analytical expression when employing LADM. With the aid of LADM, the solution's convergence is more precise and occurs more quickly. Additionally, second-order ordinary DEs can be resolved via this strategy.

6 Conclusion

The HA pandemic model was served as the basis for a mathematical investigation. By employing the LADM and TSM, the approximate analytical computations for each of the model's four compartments were found. The consequences of the many parameters in the model were illustrated graphically. By comparing the results with a numerical simulation (MATLAB) for each parameter, an ideal fit has been found. The results improve the model's comprehension for learners and highlight how specific parameters affect the populations. Essentially, LADM proved a more useful and reliable strategy for many practical problems, even if both approaches (LADM and TSM) can generate semi-analytical solutions. It was a more effective and dependable method for a variety of nonlinear DEs since it avoids the significant computational effort

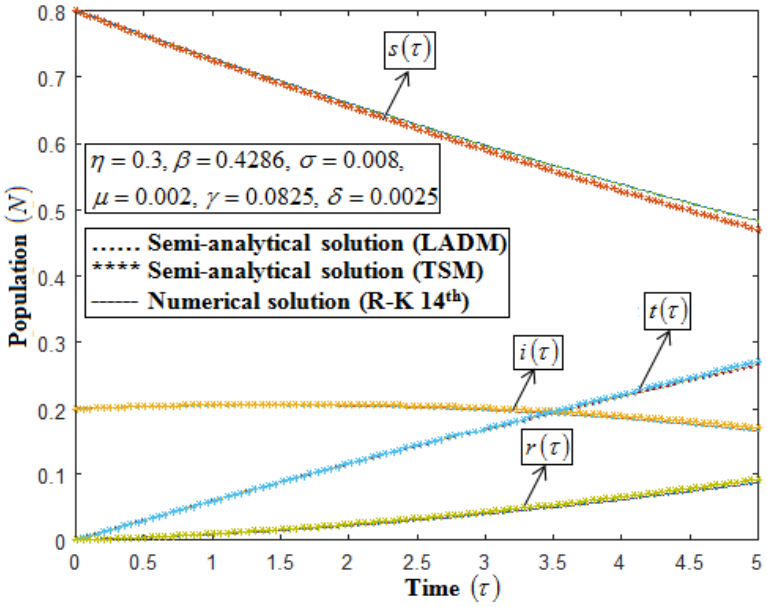

Figure 2: Comparison of approximate analytical expression with the numerical simulation for the considered epidemic model for all parameters.

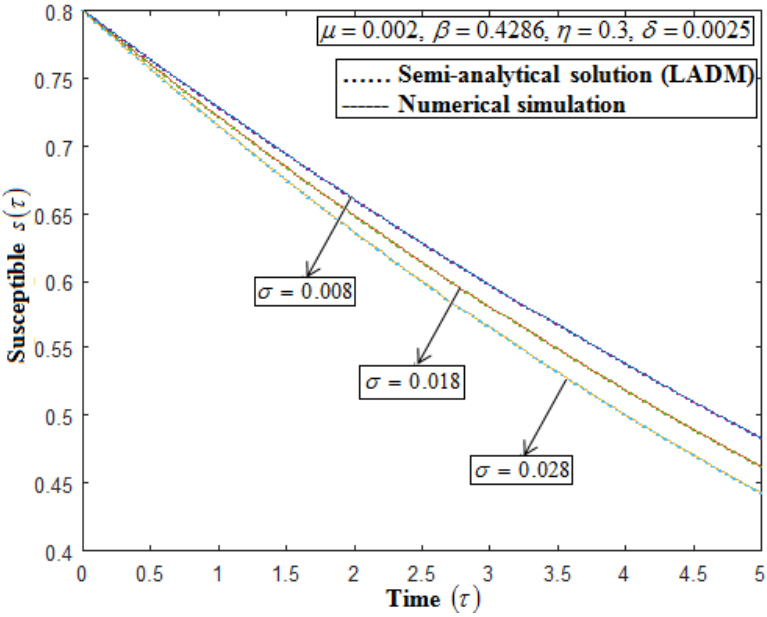

Figure 3: Curves for amount of vaccination effectiveness level σ.

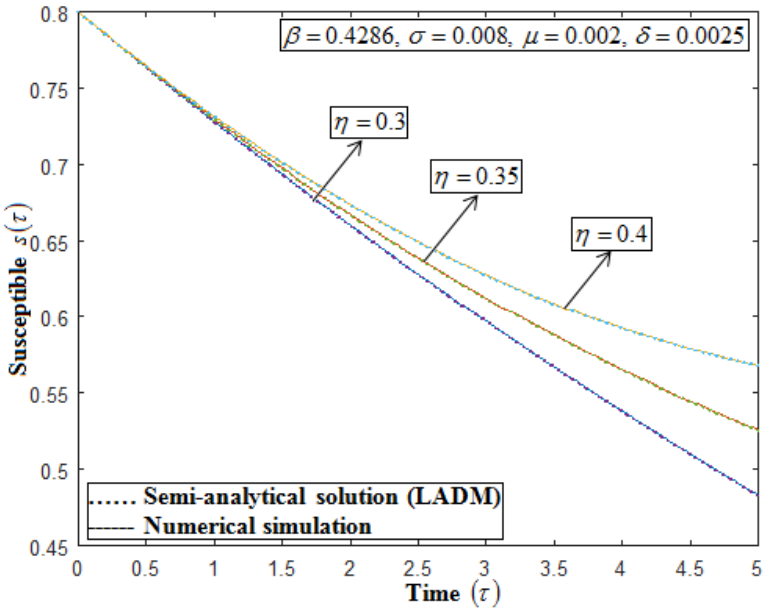

Figure 4: Consequences for proportion of infected person who receive treatment η.

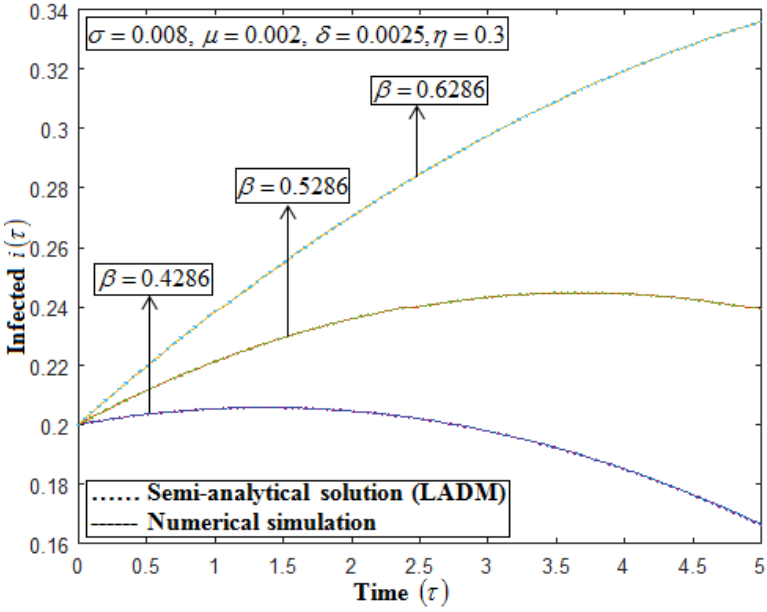

Figure 5: Influence for transmission rate of an infected individual to the suspect β.

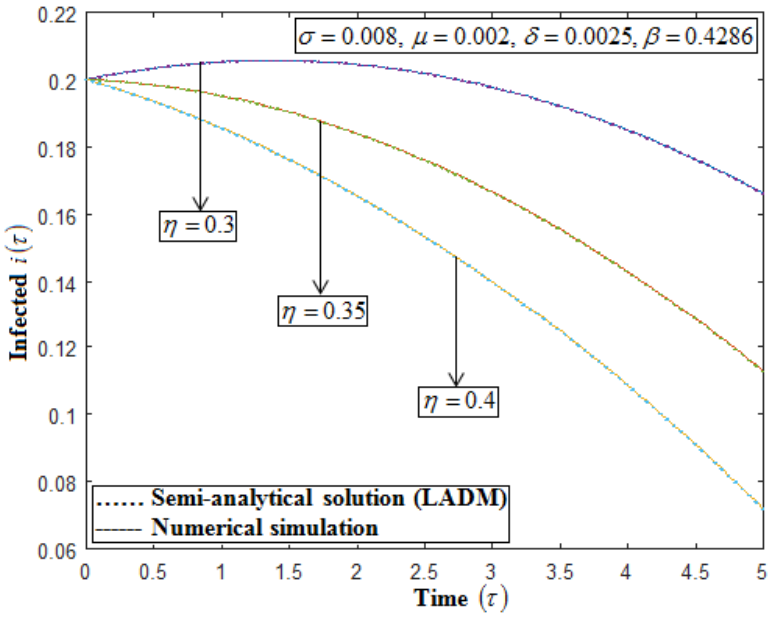

Figure 6: Plots for proportion of infected individuals who receive treatment η.

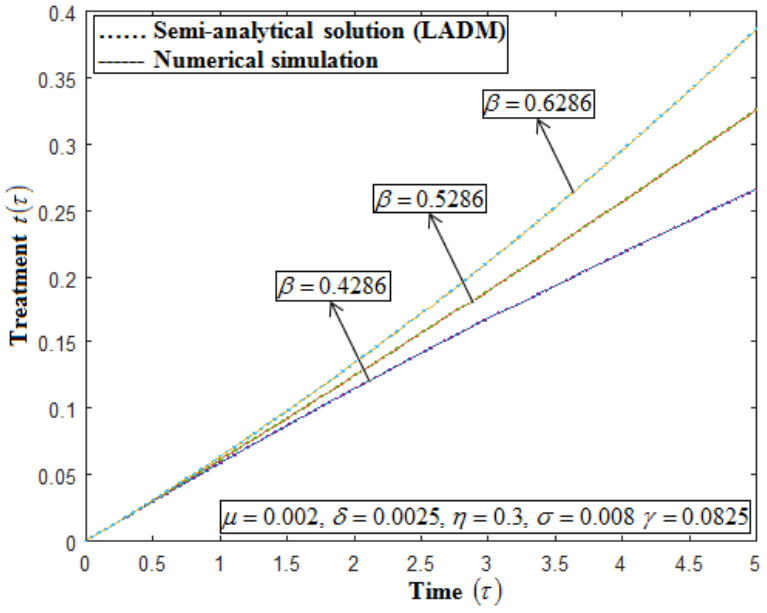

Figure 7: The impacts for transmission rate of an infected individual to the suspect β.

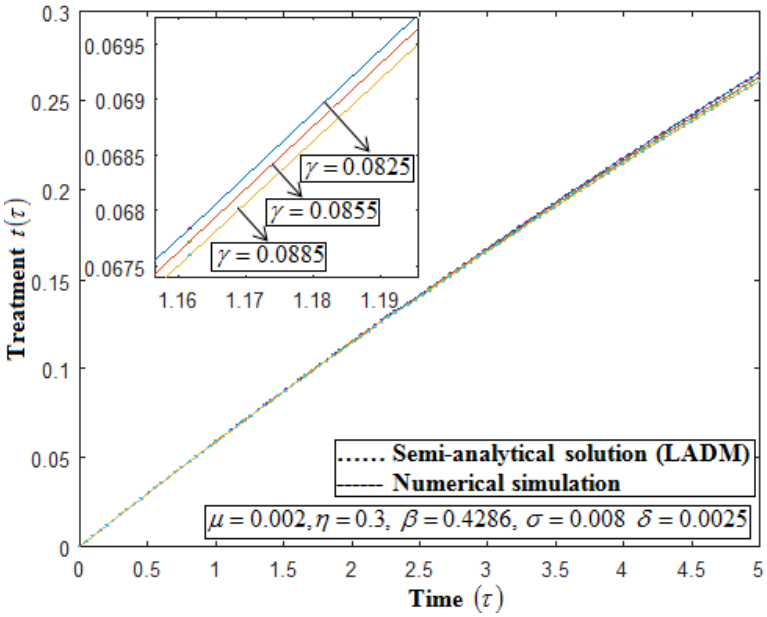

Figure 8: Influence for recovery rate of an individual after undergoing treatment for HA infection γ.

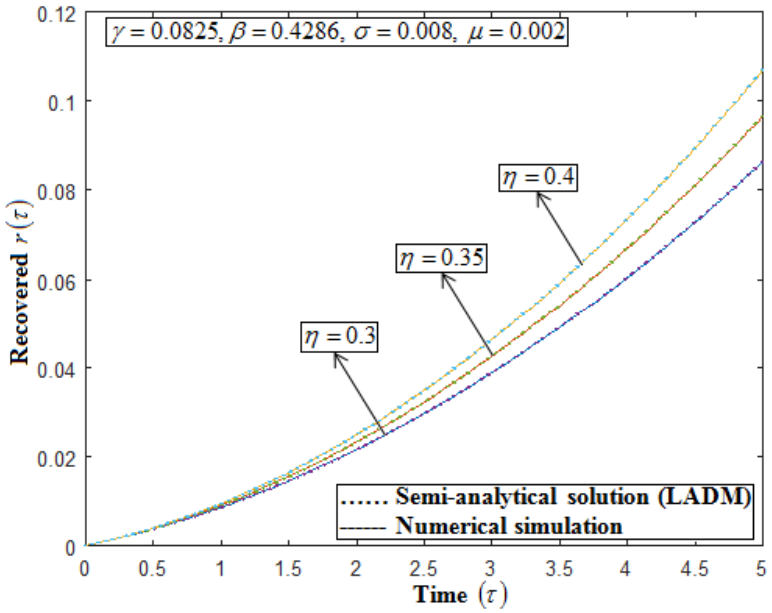

Figure 9: Consequences for proportion of infected individuals who receive treatment η.

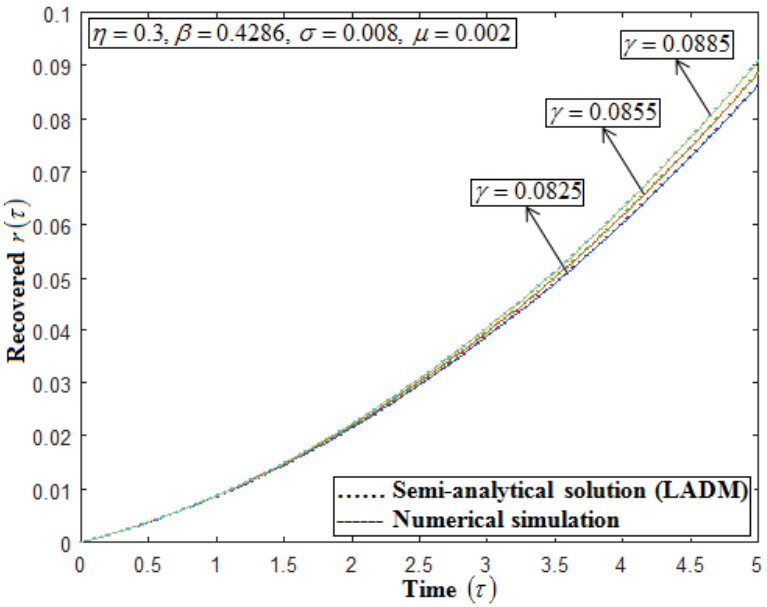

Figure 10: Impacts for recovery rate of an individual after undergoing treatment for HA infection γ.

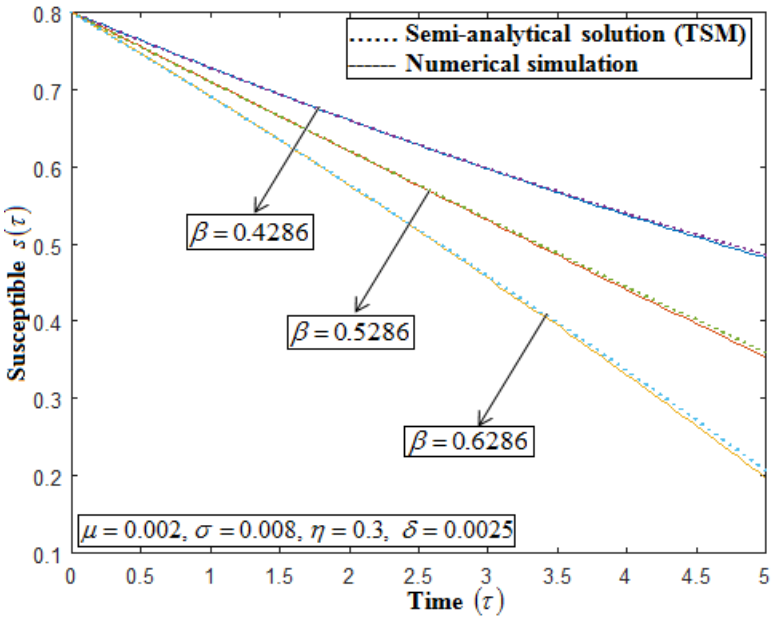

Figure 11: The impacts for transmission rate of an infected individual to the suspect β.

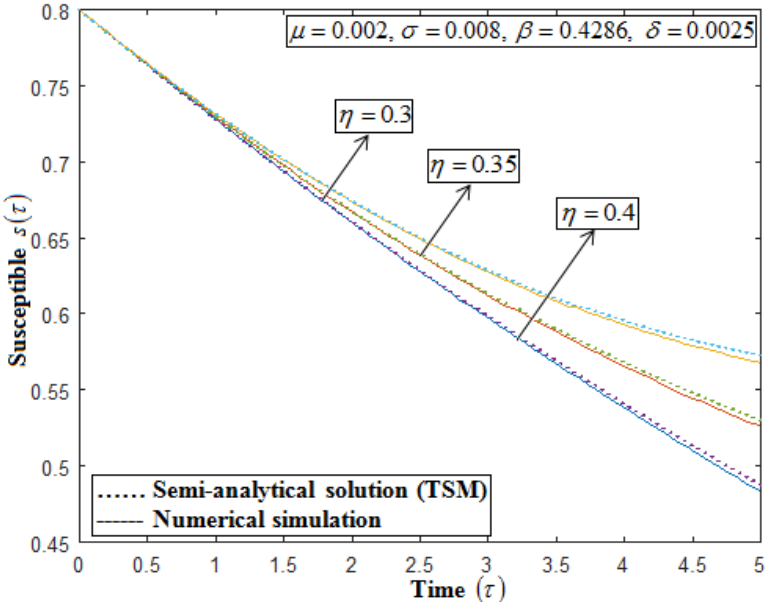

Figure 12: Consequences for proportion of infected individuals who receive treatment η.

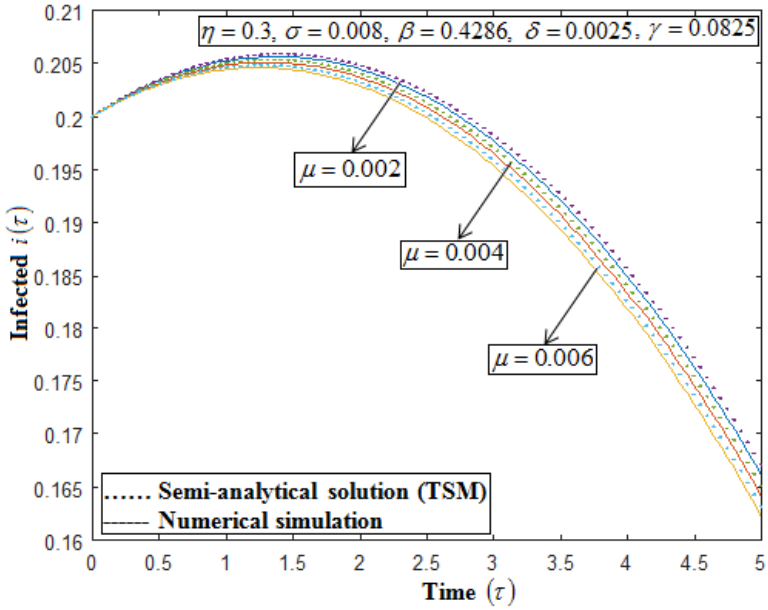

Figure 13: Variance for rate of births or deaths that are not the outcomes of HA infection (naturally) μ.

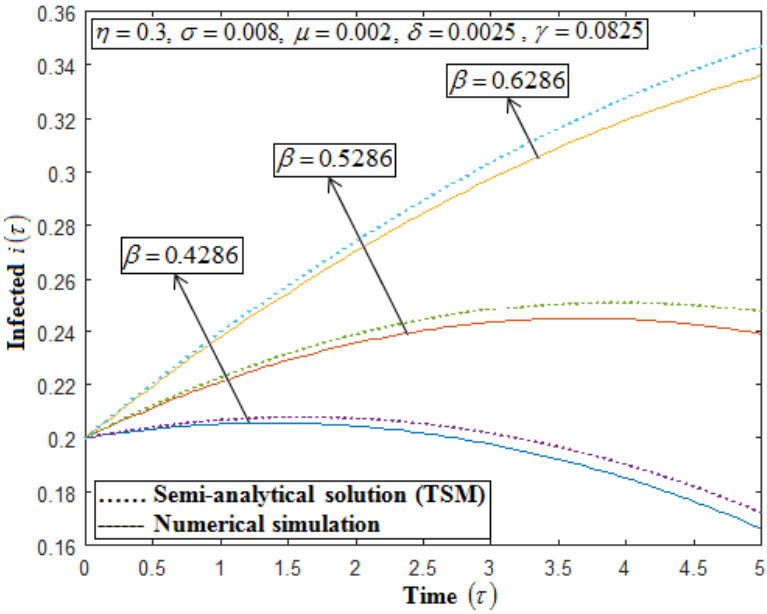

Figure 14: Plots for transmission rate of an infected individual to the suspect β.

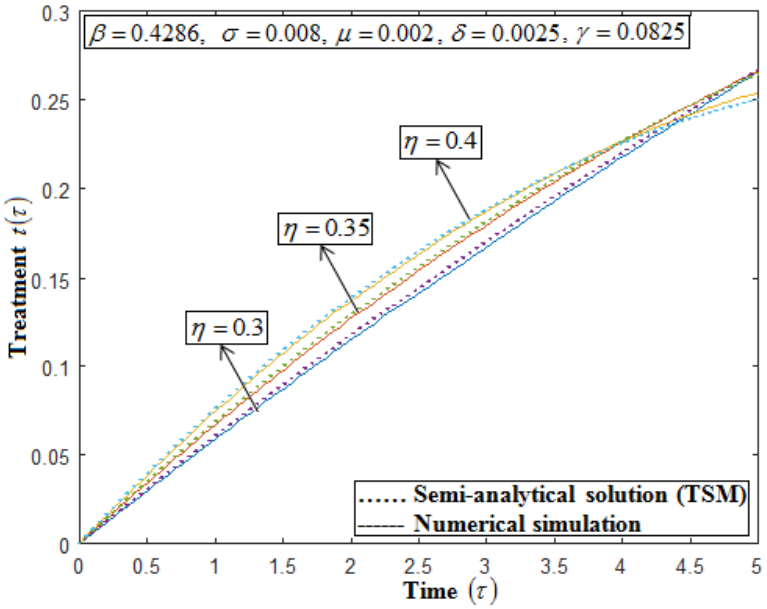

Figure 15: The effect of proportion for infected individuals who receive treatment η.

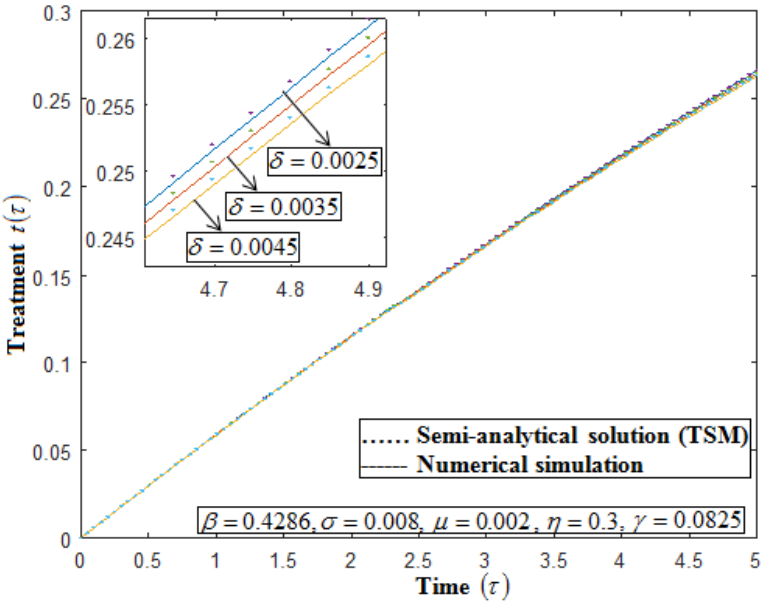

Figure 16: Influence of death rate due to HA infection δ.

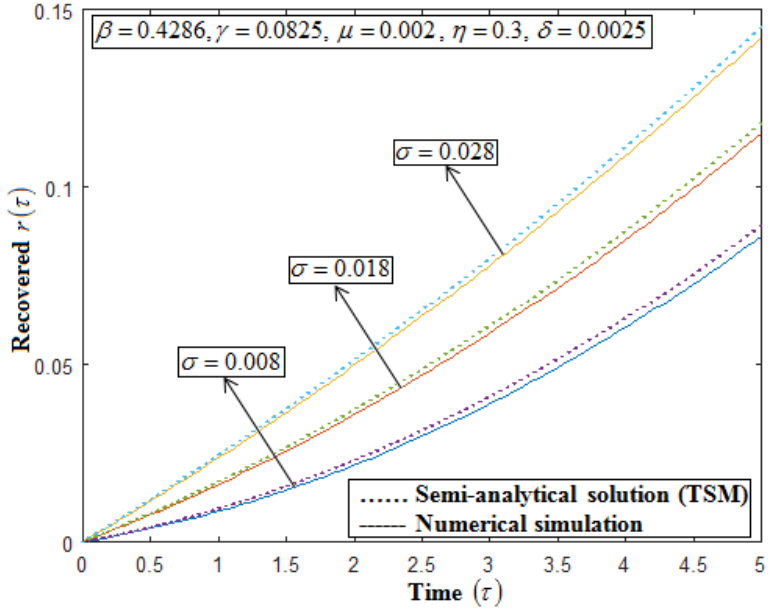

Figure 17: Variance for amount of vaccination effectiveness level σ.

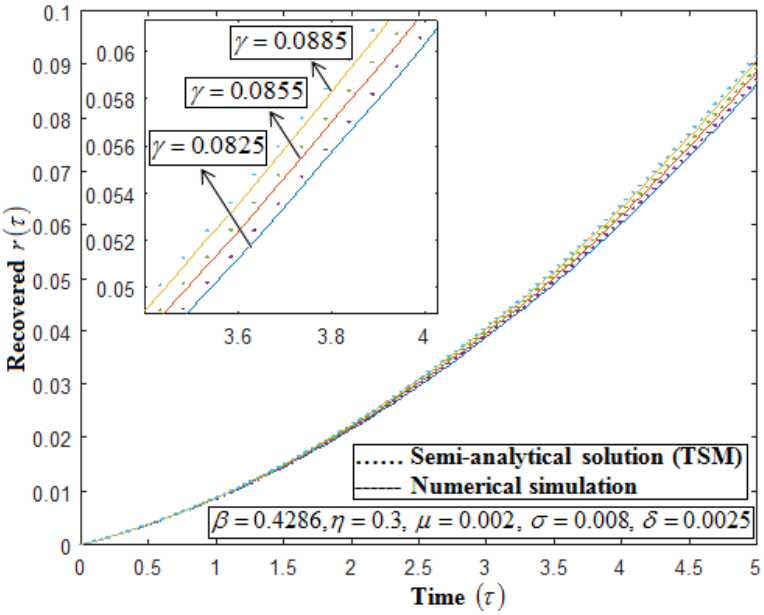

Figure 18: Impacts for recovery rate of an individual after undergoing treatment for HA infection γ.

Table 1: Contrasting numerical simulation for the susceptible class $s(\tau)$ with approximate analytical formulations for LADM and TSM with a given amount of $\mu = 0.02,\ \sigma = 0.008,\ \beta = 0.4286,\ \eta = 0.3,\ \delta = 0.0025,\ \gamma = 0.0825$.

τ	**Numerical simulation**	**LADM** (57)	**Error % of LADM**	**TSM** (77)	**Error % of TSM**
0	0.8000	0.8000	0.0000	0.8000	0.0000
1	0.7280	0.7281	0.0137	0.7283	0.0412
2	0.6602	0.6604	0.0303	0.6608	0.0909
3	0.5970	0.5970	0.0000	0.5973	0.0503
4	0.5376	0.5378	0.0372	0.5380	0.0744
5	0.4826	0.4828	0.0414	0.4830	0.0829
Absolute Average Error %			**0.0204**		**0.0566**

Table 2: The comparison of numerical simulation for the infected class $i(\tau)$ with approximate analytical formulations for LADM and TSM with an assigned value of $\mu = 0.02,\ \sigma = 0.008,\ \beta = 0.4286,\ \eta = 0.3,\ \delta = 0.0025,\ \gamma = 0.0825$.

τ	**Numerical simulation**	**LADM** (58)	**Error % of LADM**	**TSM** (78)	**Error % of TSM**
0	0.2000	0.2000	0.0000	0.2000	0.0000
1	0.2050	0.2052	0.0976	0.2055	0.2439
2	0.2042	0.2044	0.0979	0.2045	0.1469
3	0.1975	0.1977	0.1013	0.1978	0.1519
4	0.1846	0.1849	0.1625	0.1850	0.2167
5	0.1660	0.1661	0.0602	0.1663	0.1807
Absolute Average Error %			**0.0866**		**0.1567**

Table 3: Comparing numerical simulation for the treatment class $t(\tau)$ with approximate analytical formulas for LADM and TSM for a certain value of $\mu = 0.02,\ \sigma = 0.008,\ \beta = 0.4286,\ \eta = 0.3,\ \delta = 0.0025,\ \gamma = 0.0825$.

τ	**Numerical simulation**	**LADM** (59)	**Error % of LADM**	**TSM** (79)	**Error % of TSM**
0	0.0000	0.0000	0.0000	0.0000	0.0000
1	0.5860	0.5862	0.0341	0.5865	0.0853
2	0.1145	0.1145	0.0000	0.1147	0.1747
3	0.1675	0.1676	0.0597	0.1679	0.2388
4	0.2180	0.2180	0.0000	0.2182	0.0917
5	0.2655	0.2656	0.0377	0.2658	0.1130
Absolute Average Error %			**0.0219**		**0.1173**

Table 4: On contrasting the approximate analytical expressions for LADM and TSM along with the numerical simulation for recovered class $r(\tau)$ with particular amounts of $\mu = 0.02,\ \sigma = 0.008,\ \beta = 0.4286,\ \eta = 0.3,\ \delta = 0.0025,\ \gamma = 0.0825$.

τ	**Numerical simulation**	**LADM** (60)	**Error % of LADM**	**TSM** (80)	**Error % of TSM**
0	0.0000	0.0000	0.0000	0.0000	0.0000
1	0.8570	0.8572	0.0233	0.8575	0.0583
2	0.2147	0.2149	0.0932	0.2150	0.1397
3	0.3875	0.3875	0.0000	0.3877	0.0516
4	0.6035	0.6036	0.0166	0.6038	0.0497
5	0.8630	0.8631	0.0116	0.8633	0.0348
Absolute Average Error %			**0.0241**		**0.0557**

involved in locating many higher-order derivatives in TSM. As a result, LADM proved better suited for first-order nonlinear DEs with faster convergence and greater precision. Based on the findings, the following inference may be made:

- An increase in the recovery rate from HAV indicates an increase in the recovered rate as well. As a result, the disease's recovery rates aid in preventing its spread.

- As the rate of vaccination rises, so do those receiving treatment for HAV. This led us to conclude that vaccination is necessary for the affected individuals to recover.

- When vaccination rates rise, the number of people who recover from HAV infection rises, and the number of people who are susceptible that is, who are all suspected of having HAV get drops.

This led us to the conclusion that the right vaccination should be given in order to stop the spread of HAV. In order to prevent the spread of the infections, individuals should also be made aware of the importance of getting the right vaccinations and receiving treatment for HAV.

7 Appendices

Appendix A: MATLAB programming for (6) through (9)

$functiongraphmain3$
$options = odeset('RelTol', 1e-6,' Stats',' on');$
$Xo = [0.8, 0.2, 0.0, 0.0];$
$tspan = [0, 5]; ss$
tic
$[t, x] = ode45(@TestFunction, tspan, Xo, options);$
toc
$figure$
$holdon$
$plot(t, X(:, 1),' -')$
$plot(t, X(:, 2),' -')$
$plot(t, X(:, 3),' -')$
$plot(t, X(:, 4),' -')$
$legend('S',' E',' T',' R')$
$ylabel('Population')$
$xlabel('Time')$
$return$
$function[dx_dt] = TestFunction(, x)$
$mu = 0.002, delta = 0.0025, sigma = 0.008, beta = 0.4286, gamma = 0.0825, eta = 0.3;$
$dx_dt(1) = mu - (1 - sigma) * beta * x(1) * x(2) - sigma * x(1) - mu * x(1);$
$dx_dt(2) = (1 - sigma) * beta * x(1) * x(2) - eta * x(2) - delta * x(2) - mu * x(2);$
$dx_dt(3) = eta * x(2) - gamma * x(3) - delta * x(3) - mu * x(3);$
$dx_dt(4) = gamma * x(3) + sigma * x(1) - mu * x(4);$
$dx_dt = dx_dt';$
$return$

Appendix B: Nomenclature

Symbol	Meaning
β	The transmission rate of an infected individual to the suspect
t	Treatment class
γ	The recovery rate of an individual after undergoing treatment for hepatitis A infection
σ	Vaccination effectiveness level
r	Recovered class
η	Proportion of infected individuals who receive treatment
μ	Rate of births or deaths that are not the result of HA infection (naturally)
s	Susceptible class
δ	Death rate due to hepatitis A infection
i	Individuals class
τ	Time
N	The number of the human population

Conflict of interests

The authors declare that there is no conflict of interests.

Acknowledgement

The authors are very grateful to the reviewers for carefully reading the paper and for their comments and suggestions which have improved the paper. Also, the authors are thankful to Sri. S. Natanagopal, Secretary, The Madura College Board, Dr. J. Suresh, The Principal, and Dr. C. Thangapandi, Head of the Department, The Madura College (Autonomous), Madurai, Tamil Nadu, India for their constant support to our research work.

References

[1] Ajelli, M., Fumanelli. L., Manfredi, P., and Merler, S. *Spatiotemporal dynamics of viral hepatitis A in Italy*, Theor. Popul. Biol., 79 (1-2) (2011), 1–11.

[2] Ajelli, M., Iannelli, M., Manfredi, P., and Degli Atti, M.L.C. *Basic mathematical models for the temporal dynamics of HAV in medium-endemicity Italian areas*, Vaccine, 26 (13) (2008), 1697–1707.

[3] Ananthaswamy, V., Meenakshi. S., Sivasankari, S., and Seenith Sivasundaram, *A mathematical study on the transmission dynamics of Hepatitis A virus*, Math. Eng. Sci. Aerosp. (MESA), 15 (2) (2024), 613–631.

[4] Arif, M. S., Abodayeh, K., and Nawaz, Y., *Precision in disease dynamics: Finite difference solutions for stochastic epidemics with treatment cure and partial immunity*, Partial Differ. Equ. Appl. Math., 9 (1) (2024), 1–9.

[5] Ayouni, K., Naffeti, B., and W. Ben Aribi et al., *Hepatitis A virus infection in Central-West Tunisia: an age structured model of transmission and vaccination impact*, BMC Infect. Dis., 20 (1) (2020), 1–13.

[6] Bae, S. C., Park, S. Y., Kim, A. N., Oh, M. H., and Ha, S. D., *Survival of hepatitis A virus on various food-contact surfaces during 28 days of storage at room temperature*, Food Res. Int., 64 (2014), 849–854.

[7] Bazuaye, F. E. O., *A Laplace Decomposition Analysis Of Corona Virus Disease 2019 (Covid 19) Pandemic Model*, Int. J. Math. Sci. Optim.: Theor. Appl., 6 (2) (2020), 847–861.

[8] Bianco, E., Mariano, A., Mele, A., Spada, E., and Tosti, M., *Epidemiology of acute viral hepatitis: twenty years of surveillance through SEIEVA in Italy and a review of the literature*, Rapp. ISTISAN, 12 (2006).

[9] Brouwer, A. F., Zelner, J. L., and Eisenberg, M. C., et al., *The impact of vaccination efforts on the spatiotemporal patterns of the hepatitis A outbreak in Michigan, 2016–18*, Epidemiol., 31 (5) (2020), 628–635.

[10] Farman, M., Azeem, M., and Ahmad, M.O., *Analysis of COVID-19 epidemic model with sumudu transform*, AIMS Public Health, 9 (2) (2022), 316–330.

[11] Febriyanto, E.Y., and Dewi, M. F., *Numerical analysis of Hepatitis A transmission using the susceptible-infected-treatment-recovery (SITR) model with vaccination using 14th-order Runge-Kutta method Runge Kutta method*, Rangkiang Math. J., 4 (1) (2025), 6–15.

[12] Fiore, A.E., *Hepatitis A is transmitted by Food*, Clin. Infect. Dis., 38 (5) (2004),705–715.

[13] Fiore, A.E., Wasley, A., and Bell, B.P., *Prevention of hepatitis A through active or passive immunization: recommendations of the Advisory Committee on Immunization Practices (ACIP)*, MMWR Recomm. Rep., 55 (7) (2006), 1–23.

[14] Groza, G., and Razzaghi, M., *A Taylor series method for the solution of the linear initial-boundary-value problems for partial differential equations*, Computers Math. Appl., 66 (2013), 1329–1343.

[15] Guimaraens, M.A.D., and Codec, C.T., *Experiments with mathematical models to simulate hepatitis A population dynamics under different levels of endemicity*, Cadernos de Sa´ude P´ublica, 21 (5) (2005), 1531–1539.

[16] Harir, A., Melliani, S., El Harfi, H., and Chadli, L.S., *Variational iteration method and differential transformation method for solving the SEIR epidemic model*, Int. J. Differ. Equ., 2020 (1) (2020), 6314–6320.

[17] Harisma, F.B., Syahrul, F., Mubawadi, T., and Mirasa, Y. A., *Analisis Kejadian Luar Biasa Hepatitis A di SMA X Kabupaten Lamongan Tahun 2018*, J. Berk. Epidemiol., 6 (2) (2018), 112–121.

[18] He, J.H., and Ji, F.Y., *Taylor series solution for Lane-Emden equation*, J. Math. Chem., 57 (2019), 1932–1934.

[19] He, C.H., Shen, Y., Ji, F.Y., and He, J.-H., *Taylor series solution for fractal Bratu-type equation arising in electrospinning process*, Fract., 28 (2020), 2050011–2052193.

[20] Ilahi, F., and Fadilaturrohmah, N., *Model SEIR Untuk Penyebaran Penyakit Hepatitis C Dengan Pengobatan Pada Populasi Terinfeksi Kronis*, Jurnal Riset Dan Aplikasi Matematika (JRAM), 5 (1) (2021), 19–28.

[21] Jouhda, Z.M. and AL-Azzawi, S.N.A., *Analysis Approximate with Using Sumudu Adomian Decomposition Method for Solving SEIVR Epidemic Model*, J. Engin., 31 (2) (2025), 177–202.

[22] Koff, R. S., *Clinical manifestations and diagnosis of hepatitis A virus infection,* Vaccine, 10, Supplement 1, (1992), S15–S17.

[23] Krugman, S., and Giles, J.P., *Viral hepatitis: New light on an old disease*, JAMA, 212 (6) (1970), 1019–1029.

[24] Mac Kinney-Novelo, I., Barahona-Garrido, J., Castillo-Albarran, F., Santiago-Hernández, J.J., Méndez-Sánchez, N., Uribe, M. and Chávez-Tapia, N. *Clinical course and management of acute hepatitis A infection in adults*, Ann. Hepatol., 11 (5) (2012), 652–657.

[25] Meenakshi, S., Ananthaswamy, V., Anantha Jothi, J., and Seenith Sivasundaram *Mathematical analysis of COVID-19 disease in Malaysia using SIRS model*, Nonlinear Stud., 32 (2) (2025), 675–693.

[26] Meenakshi, S., Ananthaswamy, V., Anantha Jothi, J., and Santhi, V. K., *A Mathematical Study on SIR Epidemic Model During COVID-19*, Commun. Math. Appl., 15 (3) (2024), 1115–1128.

[27] Miletics, E., and Moln´arka, G., *Taylor series method with numerical derivatives for initial value problems*, J. Comput. Methods Sci. Eng., 4 (2004), 105–114.

[28] Mungkasi, S., *Variational iteration and successive approximation methods for a SIR epidemic model with constant vaccination strategy*, Appl. Math. Model. 90 (2021), 1–10.

[29] Narmatha, S., Ananthaswamy, V., Seenith Sivasundaram and Subha, M., *Semi analytical solution to a SIR model using new approach to homotopy perturbation method*, Math. Eng. Sci. Aerosp. (MESA), 13 (4) (2022), p. 1053.

[30] Sahu, I., and Jena, S.R., *SDIQR mathematical modelling for COVID-19 of Odisha associated with influx of migrants based on Laplace Adomian decomposition technique*, Model. Earth Syst. Environ., 9 (4) (2023), 4031– 4040.

[31] Shruthi, M., Ananthaswamy, V., and Seenith Sivasundaram, *A mathematical study on the typhoid disease model*, Math. Eng. Sci. Aerosp. (MESA), 15 (4) (2024), 1213–1231.

[32] Sidik, A. T. R., Sari, L. N., and Ismail, A., *Analisis Kestabilan Model SITR pada Penyebaran Penyakit Hepatitis A dengan Vaksinasi*, Res. Math. Nat. Sci., 1 (1) (2022), 1–11.

[33] Staes, C.J., Schlenker, T.L., Risk, I., Cannon, K.G., Harris, H., Pavia, A.T., Shapiro, C.N. and Bell, B.P. *Sources of infection among persons with acute hepatitis A and no identified*

risk factors during a sustained community-wide outbreak, Pediatrics, 106 (4) (2000), E54–E60.

[34] Stapleton, J.T., and Lemon, S.M., *Infectious Diseases, in (Chapter) Hepatitis A and hepatitis E*, Lippincott Co, Philadelphia, US, (1994), 790–797.

[35] Trujillo-Ochoa, J.L., Viera-Segura, O., and Fiery, N.A., *Challenges in management of hepatitis A virus epidemiological transition in Mexico*, Ann. Hepatol., 18 (1) (2019), 14–22.

[36] Van Effelterre, T., Marano, C., and Jacobsen, K.H., *Modeling the hepatitis A epidemiological transition in Thailand*, Vaccine, 34 (4) (2016), 555–562.

[37] Van Effelterre, T., Zink, T.K., Hoet, B.J., Hausdorff, W.P., and Rosenthal, P., *A mathematical model of hepatitis A transmission in the United States indicates value of universal childhood immunization*, Clin. Infect. Dis., 43 (2) (2006), 158–164.